# Numerical Analysis of Geogrid-Axial Stiffness on Shear Strength Behavior of Fine Sand

## Essam badrawi*

*Structural Engineering Department, Faculty of Engineering, Zagazig University, Zagazig, Egypt*

**A R T I C L E   I N F O**

**A B S T R A C T**

One of the most popular methods for improving weak soil properties is soil reinforcement with geogrid-layers, the geogrid-layer increases the low shear resistance of fine sand. The Abaqus 3-D model is utilized to simulate large-scale direct shear apparatus. Numerical models are conducted on geogrid-reinforced fine sand to estimate how geogrid-axial stiffness affects the shear strength behavior. Shear parameters, shear strength ratio, internal shear coefficient, and mobilized geogrid tensile strength are studied in both longitudinal and transverse directions. The steel box for large-scale direct shear consists of two separate parts with dimensions of 200 mm x 200 mm x 100 mm. A geogrid-layer with different axial stiffness between 200 kN/m and 1000 kN/m with an increment of 100 kN/m is fixed between the two separate parts to estimate the shear resistance increase of geogrid-reinforced fine sand. The shear strength of geogrid-reinforced fine sand increases with geogrid-axial stiffness; for the fine-sand elastic modulus of 10 MPa, the shear strength ratio (SSR) increases from 1.80 to 3.10 when the geogrid-axial stiffness increases from 200 kN/m to 1000 kN/m. However, the (SSR) values decreased with increasing fine-sand elastic modulus, the (SSR) values were 1.0 and 1.60 for the variation of geogrid-axial stiffness from 200 kN/m to 1000 kN/m when the fine-sand elastic modulus increased to 40 MPa. The most economical and optimal values of geogrid-axial stiffness are 500 kN/m and 300 kN/m for fine-sand elastic moduli of 10 MPa and 40 MPa, respectively.

## 1. Introduction

It is required to evaluate the shearing resistance of geogrid-reinforced fine sand for geotechnical applications such as geogrid-reinforced embankments, retaining walls, geogrid-reinforced earth fills, roads, and shallow foundations. A direct shear test is the most widely used test to determine the shearing resistance of fine sand. The shea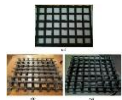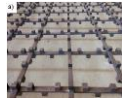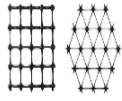r resistance of geogrid-reinforced fine sand was investigated through both numerical and experimental studies. Numerical analysis is the most suitable tool to determine parameters of geogrid-reinforced soil that were difficult to measure in experimental studies Ahad and Asghar (2009). Tamassoki (2018) presented a numerical simulation of a large-scale direct shear with different dimensions of steel boxes. The scale effect on the shear resistance of two-layer soil reinforced with a geogrid-layer is
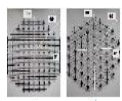
_____
* Corresponding author. Tel.: +2-01286084383
*E-mail address*: e.f.b.attia@gmail.com

investigated. The numerical results of the model agree well with the experimental results under the same test conditions. The shear resistance of geogrid-reinforced soil increases with steel box size. The shear resistance of geogrid-reinforced fine sand at interface surface between the geogrid-layer and fine sand depends on the shape of the geogrid opening. Makkar (2017) demonstrated that the interface shear resistance of fine sand was increased by 16% and 22% when the 3D triangle and rectangle geogrid-layer patterns were used, respectively. Chen (2009) presented an experimental study to determine the influence of transverse-ribs on the interface shear resistance. The transverse-ribs of the geogrid-layer provide 10% of the shear resistance of the sand-geogrid interface. The shear resistance increases depending on the geogrid aperture size, vertical stresses, geogrid tensile strength and stiffness. The friction and interlocking between soil and geogrid-layer are responsible for the shearing resistance of reinforced sand. Elkorashy (2020) investigated experimentally and numerically how cubic-cogs affect the friction and interlocking between soil and geogrid-layer. Cubic-cogs are arranged on both sides of the geogrid-ribs of the traditional biaxial geogrid-layer to increase the soil-geogrid interaction and the interlocking between geogrid-ribs and soil. The geogrid-layer with cubic-cogs increases shearing resistance by 50% and 453% and increases the friction angle by 13.52° and 42.49° compared to typical biaxial geogrid and solid steel plate, respectively. Tiwari (2022) studied how the polypropylene fiber affects the shearing resistance between expansive soil and geogrid-layer with triaxial and biaxial aperture shapes. A large-scale direct shearing box with dimensions of 300 mm × 300 mm × 150 mm is used in the study. The angle of shearing resistance increased from 8.44° to 21.23°, the cohesion value increased from 52.61 kPa to 93.89 kPa and the shearing resistance of expansive soil increased from 55.43 kPa to 154 kPa for biaxial and triaxial geogrid, respectively. Stacho (2020) studied the effect of geogrid thickness ($h_{geogrid}$), geogrid aperture size ($L_{geogrid}$), and soil particle sizes at 50% of the percentage passing ($d_{50}$) on shearing resistance. The experimental work is carried out on three soil samples with different particle sizes, the three samples are poorly graded sand, poorly graded fine gravel, and poorly graded medium gravel. The adhesion values between sand and geogrid increase 3.68 times compared to unreinforced sand. The maximum shearing resistance occurs at a ratio of 5.0 for both $L_{geogrid}/d_{50}$ and $d_{50}/h_{geogrid}$. Ferreira (2015) describes an investigation of the influence of moisture content, soil

unit weight, and geosynthetic type on the interface-shearing resistance of the soil-geosynthetic. The interface-shear resistance decreases with increasing moisture content. The reduction of the interface-shearing resistance is 20%, 22%, and 27% for the water content increases from dry state to 0.50 of the optimum moisture content, from 0.50 $W_{opt}$ to $W_{opt}$, and $W_{opt}$ to 1.50 $W_{opt}$, respectively. Zhang (2021) studies the shear directions and geogrid aperture shapes on the shearing resistance of reinforced soil. The shearing tests were carried out for three different biaxial geogrids and triaxial geogrids under the shear directions of 0°, 45°, and 90°. The variation of shearing resistance is 59.59% for the soil-biaxial-geogrid interface and 37.99% for the soil-triaxial-geogrid interface. The shear strength ratio (SSR) is defined as the ratio between the shearing resistance of reinforced soil and unreinforced soil. Table (1) lists the maximum values of shear strength ratio (SSR) from the previous studies.

Table 1. large-scale direct shear test results

| Name | Shear Strength Ratio, SSR | Geogrid Photo | Geogrid Shape | Soil type |
|---|---|---|---|---|
| Makkar, (2017) | 1.22 |  | 3D Geogrid | Fine sand and med. sand |
| Elkorashi, (2020) | 6.0 |  | Isometric Cogged Biaxial Geogrid, | sand |
| Tiwari, (2022) | 2.98 |  | Biaxial and Triaxial geogrid | Expansive clay |
| Stacho, (2020) | 1.30 |  | Geogrid size (25x25, 40x40) | Sand, fine gravel and med gravel |
| Zhang, (2021) | 1.41 |  | Geogrid specimen and shear direction | fine sand, coarse sand, and gravel |

This research presents a numerical simulation of large-scale direct shearing test to evaluate the effect of geogrid-axial stiffness on the shearing resistance of geogrid-reinforced fine sand in both longitudinal and transverse directions. In addition, the shearing strength parameters and the mobilized tensile strength of geogrid-ribs in both directions are also evaluated.

## 2. Numerical Model

The fine sand is one of the soil types with low shear strength values and the geogrid-layer provides an increase in fine-sand shearing resistance. A large-scale direct shear test is simulated using Abaqus software (Ver. 2017) to evaluate the effect of geogrid-axial stiffness (J) on the fine-sand shearing strength. In the simulation model, the fine sand is subjected to vertical stresses varying between 25 kPa and 100 kPa with an increment of 25 kPa. A horizontal displacement of 10 mm is applied to the upper direct shearing box until the fine sand fails. The elastic modulus of fine sand used in the 3-D simulation is 10 MPa and 40 MPa, the fine sand properties are listed in Table (2). The geogrid-axial stiffness (J) depends on the geogrid elastic modulus, thickness, tensile strength and strain as described in Equation (1).

$$J = T/\varepsilon = E \ x \ t \qquad (1)$$

Where:

        J = Geogrid-axial stiffness, kN/m,
        T = Geogrid tensile strength, kN/m
        E = Geogrid elastic modulus, kPa,
        $\varepsilon$ = Geogrid strain
        t = Geogrid thickness, m

Table 2. Fine Sand Properties

| Property | Symbol | Fine Sand | Steel Box |
|---|---|---|---|
| Unit weight, (kN/m³) | $\gamma$ | 18.0 | 78 |
| Poisson ratio | $\upsilon$ | 0.35 | 0.15 |
| Elastic modulus, MPa | E | 10 and 40 | $2.1e^5$ |
| Material Cohesion, (kPa) | d* | 0.01 | -- |
| Friction angle, (º) | $\phi$ | 30 | -- |
| | $\beta$* | 50.19 | |
| Cap Eccentricity | R | 0.72 | -- |
| Ini. cap yield surface posit. | -- | 0.056 | -- |
| Trans. surface radius | $\alpha$ | 0.10 | -- |
| Flow Stress Ratio | k | 0.9 | -- |

* $\tan\beta = \dfrac{6 \ x \sin\phi}{3 - \sin\phi}$ , $d = \dfrac{18 \ x \ C \ x \cos\phi}{3 - \sin\phi}$

In the simulation model, the geogrid-axial stiffness varies between 200 kN/m and 1000 kN/m, the geogrid thickness is constant and the geogrid-layer elastic modulus is varying to achieve the required values of axial stiffness for each case. The geogrid-layer is biaxial with aperture size of 45 mm x 45 mm, the geogrid thickness is 2.0 mm and the width of geogrid-ribs in the longitudinal and transverse directions is 5.0 mm. The properties of geogrid-layer are listed in Table (3). The numerical model consists of a steel box (upper and lower parts), fine sand and a geogrid-layer. The lower steel part is filled with fine sand and geogrid-layer is fixed to the lowered part. The openings in the geogrid-layer are filled with fine sand to achieve interlocking at the contact surface. The upper steel part is then placed over the lower part and filled with fine sand. The normal stress is applied to the top of the fine sand and the horizontal displacement is gradually applied to the upper part of the steel box until failure occurs. The contact interface between fine sand and the geogrid-layer is defined by friction coefficient ($\mu$), which is assumed to be 0.90. The geogrid-layer and the steel box were modeled as a linear-elastic material and the fine sand was assumed to be an elastic-plastic material by a modified Drucker-Prager model with a hardening curve. The hardening curve of cap plasticity model is the volumetric strain and pressure relationship. Park and Byrne (2004) describe an equation to represent the hardening curve as described in Equation (2).

$$\varepsilon_v = \frac{2x(1.5 - D_{ro})}{C} \sqrt{\frac{P}{P_{atm}}} \qquad (2)$$

Where:

        $\varepsilon_v$ = volumetric strain, %,
        $D_{ro}$ = initial relative density, %,
        C = material constant,
        P = mean stress, kPa,
        $P_{atm}$ = atmospheric pressure, kPa

The simulated boundary conditions have an impact on the shear strength results. A numerical model is carried out in three steps: the initial, normal and shearing steps. The bottom surface of the steel box and fine sand are constrained in all steps in X, Y and Z directions, the side wall of lower steel part is constrained in all steps in X and Y directions. The top of the model and side wall of upper steel part are constrained in X and Y directions in the initial and normal steps and then move in Y direction in a shearing step of 10 mm. The steel box, geogrid-layer and fine sand were modeled using C3D8R (8-node linear-brick, reduced integration, hourglass control). Figure (1) shows a large-scale direct shearing test and geogrid dimensions. Figure (2) shows horizontal displacement shading of geogrid-reinforced fine sand. Figure (3)

shows shearing resistance shading in the loading direction. Table (4) shows the Parametric study.

Table 3. Geogrid-layer Properties.

| Properties | Value |
|---|---|
| Shape of aperture | Biaxial |
| Aperture size | 45 mm × 45 mm |
| rib thickness | 2.0 mm |
| rib width | 5.0 mm |
| Ult. tensile strength ($T_{ult}$) | 30 kN/m |
| Axial stiffness, kN/m | Varied from 200 to 1000 |
| Unit weight, (kN/m³) | 7.0 |

Table 4. Shear strength Parametric study

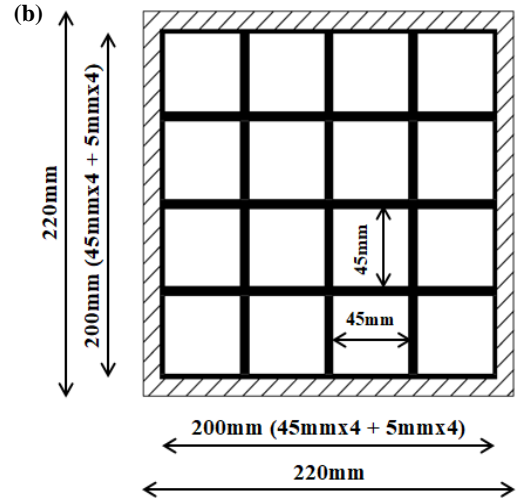| Shear Direction | Fine Sand Elastic Modulus, MPa | Normal Stress, kPa | Geogrid-Axial Stiffness, kN/m |
|---|---|---|---|
| Longitudinal Direction | 10 | 25 | 200, 300,400, 500, 600, 700, 800, 900, 1000 |
| | | 50 | |
| | | 75 | |
| | | 100 | |
| | 40 | 25 | 200, 300,400, 500, 600, 700, 800, 900, 1000 |
| | | 50 | |
| | | 75 | |
| | | 100 | |
| Transverse Direction | 10 | 25 | 200, 300,400, 500, 600, 700, 800, 900, 1000 |
| | | 50 | |
| | | 75 | |
| | | 100 | |
| | 40 | 25 | 200, 300,400, 500, 600, 700, 800, 900, 1000 |
| | | 50 | |
| | | 75 | |
| | | 100 | |



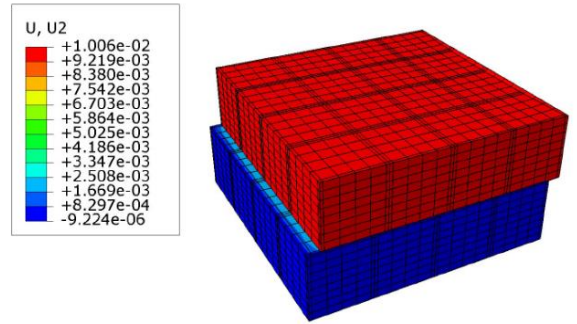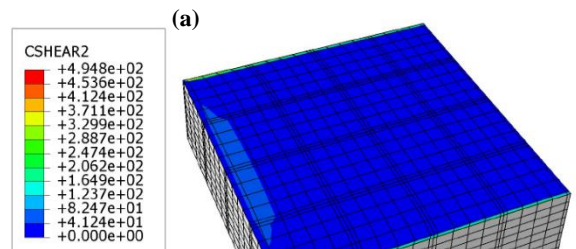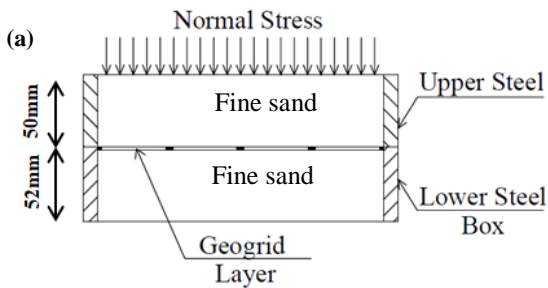Fig. 1. Large-Scale Direct Shear Test and Geogrid Dimensions.



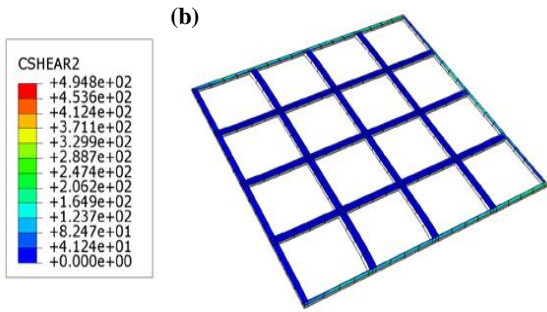Fig. 2. Horizontal Displacement Shading of reinforced Fine Sand.

**(b)**

Fig. 3. Shear Strength Shading in the Loading Direction.

## 3. Numerical Results

### 3.1. Model Verification

Anubud (2023) presents an experimental study to estimate the effect of a para-rubber sheet geogrid-layer on the shear strength of three soil types: clay, sand, and lateritic soil. In the experimental study, the large-scale direct shear test with a dimensions of 305 mm in length, 305 mm in width and 50 mm in height is used. In this study, the experimental model developed by Anubud (2023) was used to evaluate the efficiency of the numerical model developed for the large-scale direct shear test, the test is carried out on unreinforced and reinforced sand soil under normal stresses of 30, 60, and 120 kPa. The soil properties are: $E_{soil}$ = 20 MPa, $\nu$ = 0.35, C = 2.89 kPa, $\phi$ = 24.48 degrees, dry unit weight = 19.0 kN/m³, while the geogrid-layer properties are: aperture size = 20 x 20 mm, thickness = 2.38 mm, and geogrid-axial stiffness = 330 kN/m. For sandy soil, the experimental results of Anubud (2023) are used to validate the results of the numerical model. The shearing resistance values of unreinforced sand from the experimental study are 17.44, 28.71, and 57.81 kPa when subjected to normal stresses of 30, 60, and 120 kPa, respectively. Furthermore, the shearing resistance values from the Abaqus simulation model are 16.66, 30.2, and 56.61 kPa at the same values of normal stresses as described in Figure (4). The variation of shearing resistance from the experimental study and numerical model varies between 4.47% and 2.07% for the normal stress increase from 30 kPa to 120 kPa. The results of the simulation model agree well with the experimental results; the numerical model is considered a valuable tool for determining the shearing resistance of unreinforced fine sand. The Abaqus simulation model is used to evaluate the shearing resistance behavior of geogrid-reinforced fine sand and

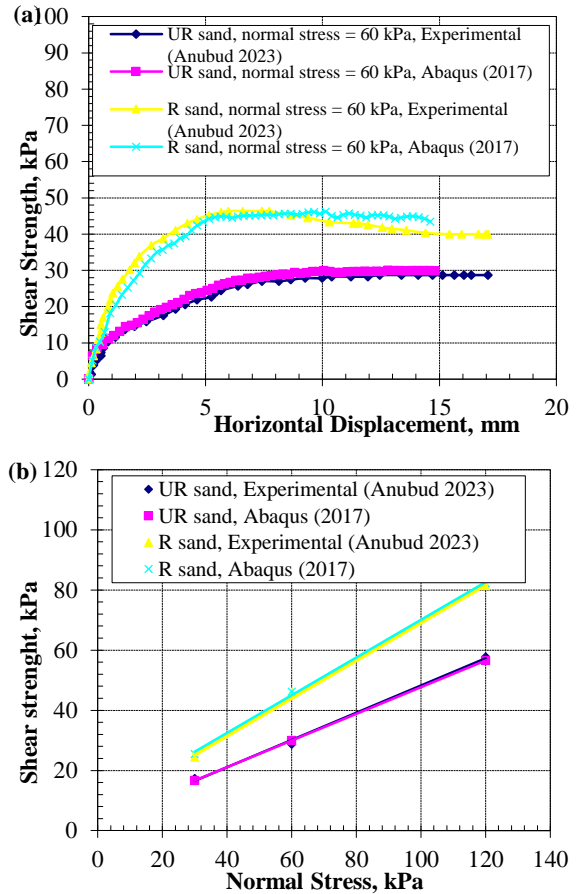investigate the influence of the axial stiffness of the geogrid-layer.



**(a)**



**(b)**

Fig. 4. Shear Strength Results of Unreinforced and Reinforced Fine Sand.

### 3.2. Longitudinal Direction

In direct shear simulation, the steel box consists of two parts: upper and lower parts. In the shearing step, the upper part of the steel box moves in the Y direction until shear failure occurs. The direction in which the upper part of the steel box moves is called the longitudinal or loading direction, the other direction is called the transverse direction (X direction).

### 3.2.1. Shear Strength Behavior

Due to the interlocking between soil particles and the geogrid-layer at the contact surface, the geogrid-layer plays an essential role in increasing the fine-sand shearing resistance. The fine-sand elastic modulus and the axial stiffness of the geogrid have a noticeable influence on the degree of interlocking. Figure (5) shows the shearing resistance behavior of unreinforced

and reinforced fine sand. The shearing resistance values of unreinforced fine sand are 15.27, 30.19, 44.32 and 60.20 kPa at normal stresses of 25, 50, 75, and 100 kPa, respectively. The shearing resistance values for the fine-sand elastic modulus of 10 MPa are 32.49, 57.51, 83.85 and 127.6 kPa when geogrid-axial stiffness is 200 kN/m, while the values are 44.5, 67.16, 108.16 and 147.26 kPa for the geogrid-axial stiffness of 1000 kN/m with the same normal stress values. For fine-sand elastic modulus of 40 MPa, the shearing resistance values are 19.68, 38.24, 54.32 and 79.97 kPa for geogrid-axial stiffness of 200 kN/m and 25.34, 42.12, 57.35, and 67.45 kPa for geogrid-axial stiffness of 1000 kN/m at normal stresses of 25, 50, 75, and 100 kPa, respectively. The numerical results for the two cases of fine-sand elastic modulus demonstrate that shearing resistance values increase with geogrid-axial stiffness and are considered more effective at low elastic modulus and low normal stresses.
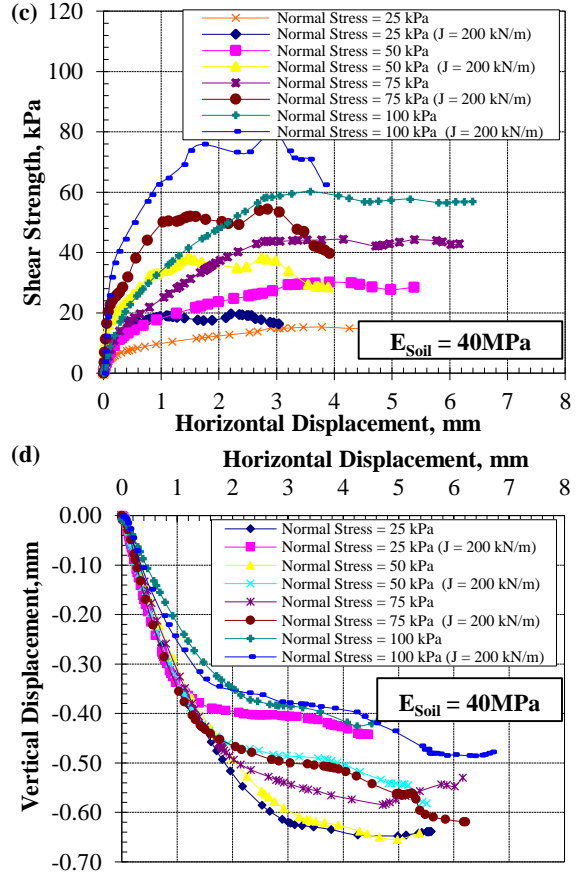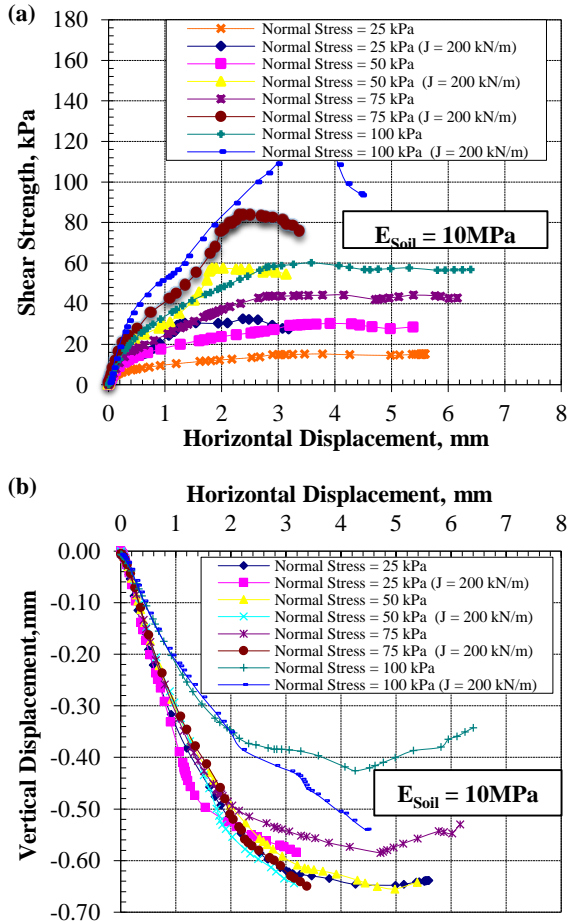
**(a)**

**(b)**

**(c)**

**(d)**

Fig. 5. Numerical Shear Strength of reinforced and unreinforced fine sand in longitudinal Direction.

### 3.2.2. Shear Strength Parameters

Figure (6) shows the shearing resistance parameters of reinforced fine sand with different geogrid-axial stiffness when the fine-sand elastic modulus is 10 MPa and 40 MPa. The friction angle at the contact surface of unreinforced fine sand is 30.32° for elastic moduli of 10 MPa and 40 MPa. As shown in Figure (6-a), the angle of friction decreases with the increasing of geogrid-axial stiffness and fine-sand elastic modulus. The friction angles of reinforced fine sand with geogrid-axial stiffness of 200 kN/m are 51° and 38° for fine-sand elastic modulus of 10 MPa and 40 MPa, respectively; these values are 44.3° and 26.51° for geogrid-axial stiffness of 1000 kN/m. The adhesion between the fine sand and geogrid-layer increases with the geogrid-axial stiffness and decreases with the fine-sand elastic modulus. The adhesion values for a fine-sand elastic modulus of 10 MPa increase from 0 to 18.28 kPa with the geogrid-axial stiffness increases from 200 kN/m to 1000 kN/m. In addition to a fine-

sand elastic modulus of 40 MPa, the adhesion values increase from 0 to 16.29 kPa with the same values of geogrid-axial stiffness.
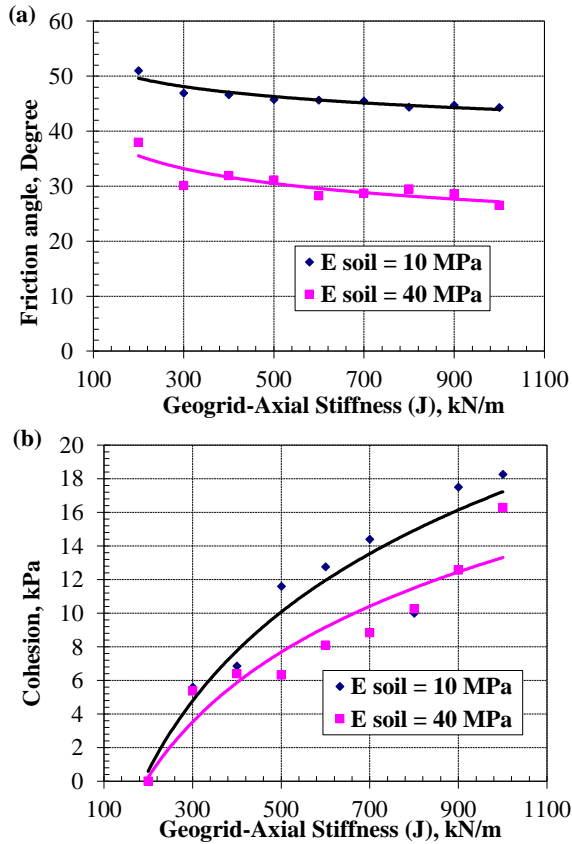


Fig. 6. Shear Strength Parameters versus Geogrid-Axial Stiffness in the longitudinal Direction.

### 3.2.3. Shear strength Ratio

Shear strength ratio (SSR) is defined as the ratio between the shearing resistance of reinforced and unreinforced fine sand. The (SSR) value describes the degree of improvement in fine-sand shearing resistance. Figure (7) shows the relationship between the (SSR) values and geogrid-axial stiffness (J) at different values of normal stress and fine-sand elastic modulus. At a normal stress of 25 kPa and a fine-sand elastic modulus of 10 MPa, the (SSR) value increases from 2.25 to 3.08 when the geogrid-axial stiffness varies between 200 and 1000 kN/m, the (SSR) value increases from 2.11 to 2.55 when the normal stress is 100 kPa with the same values of geogrid-axial stiffness. As shown in Figure (7-b), the (SSR) value decreases with the increasing of fine-sand elastic modulus at the same values of geogrid-axial stiffness and normal stress. The use of a geogrid-layer to improve the fine-

sand shear strength is more efficient at low values of elastic modulus and geogrid-axial stiffness and also minimizes the cost of the soil improvement method.
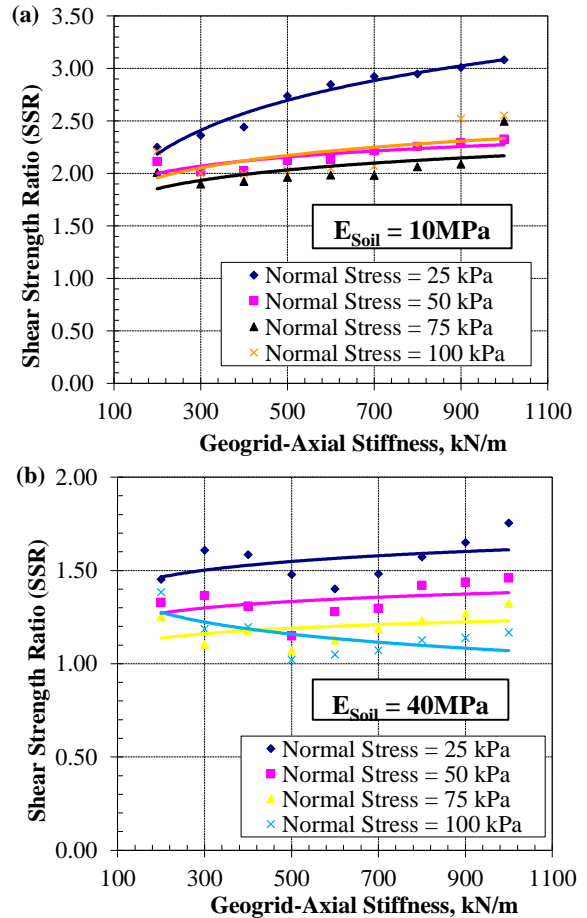


Fig. 7. Shear Strength Ratio (SSR) versus Geogrid-Axial Stiffness in longitudinal Direction.

### 3.2.4. Interface Shear Strength Coefficient

The interface shear strength coefficient ($\mu$) is described as the ratio between the maximum shearing resistance of reinforced fine sand and the applied normal stress. Figures (8) illustrate the relationship between the interface shear strength coefficient and geogrid-axial stiffness under normal stresses of 25, 50, 75, 100 kPa, the fine-sand elastic moduli are 10 MPa and 40 MPa. The results show the interface shear strength coefficients at a normal stress of 25 kPa and a fine-sand elastic modulus of 10 MPa are 1.28 and 1.78 for the geogrid-axial stiffness of 200 kN/m and 1000 kN/m, respectively, these values are 0.84 and 1.01 for the fine-sand elastic modulus of 40 MPa. The values of the interface shear strength coefficients decrease as the fine-sand elastic modulus increases. based on the

results, the most optimum and economical values of geogrid-axial stiffness are 500 kN/m and 300 kN/m for a fine-sand elastic modulus of 10 MPa and 40 MPa, respectively.
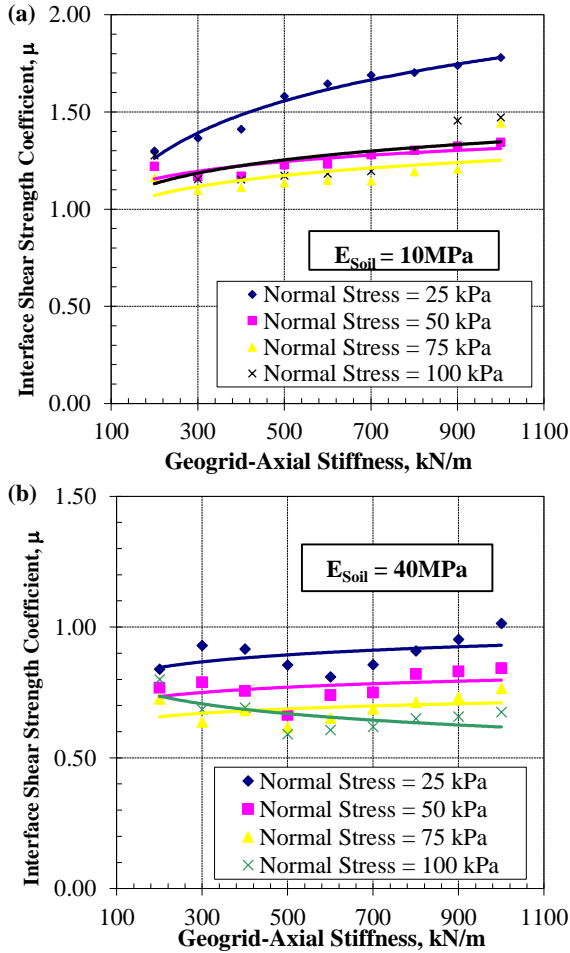


Fig. 8. Interface Shear Strength Coefficient versus Geogrid-Axial Stiffness in longitudinal Direction.

### *3.2.5. Mobilized Geogrid Tensile Strength*

The geogrid tensile strength defines the maximum load that the geogrid can withstand before failure or large strain occurs. the geogrid tensile strength used in the numerical analysis is 30 kN/m. Figure (9) shows the mobilized tensile strength developed within the geogrid-ribs in the loading direction for the two cases of fine sand with elastic moduli of 10 MPa and 40 MPa. The mobilized tensile strength values increase with the geogrid-axial stiffness and fine-sand elastic modulus at different values of normal stresses. For a fine-sand elastic modulus of 10 MPa and a normal stress of 100 kPa, the mobilized tensile strength values are 9.16

kN/m and 18.0 kN/m for geogrid-axial stiffness of 200 kN/m and 1000 kN/m, respectively. Furthermore, the mobilized tensile strength is 5.92 kN/m and 11.60 kN/m when the fine-sand elastic modulus increases to 40 MPa under the same conditions. The results illustrate that all mobilized values of tensile strength are smaller than the ultimate tensile strength and more efficient for the lower values of fine-sand elastic modulus.
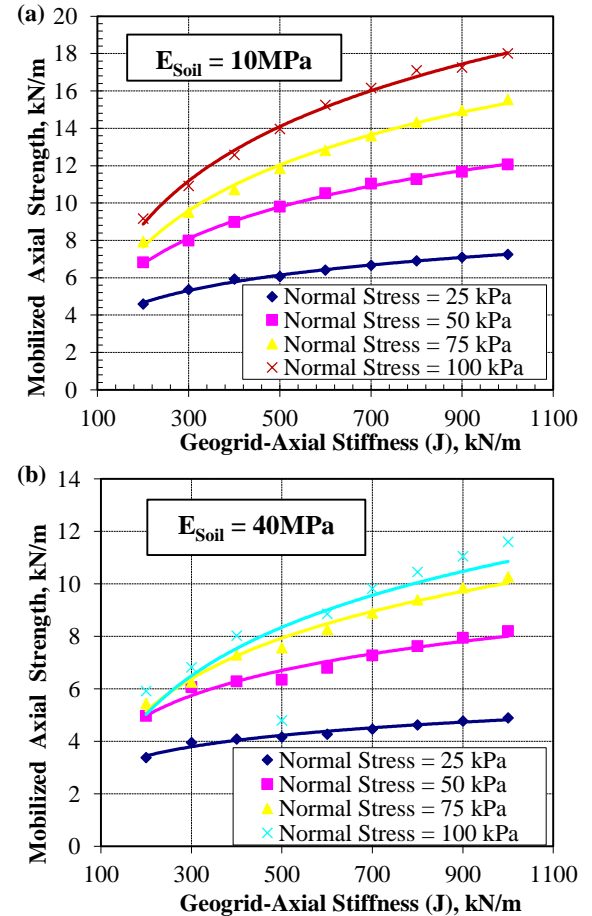


Fig. 9. Mobilized Geogrid Axial Strength versus Geogrid-Axial Stiffness in longitudinal Direction

### *3.3. Transverse Direction*

The dimensions of the biaxial geogrid-layer used in the analysis are 45 mm x 45 mm with a constant thickness of 2.0 mm, and the geogrid-ribs have a constant width of 5.0mm in both directions. The transverse-ribs transmit part of the shearing forces mobilized at the contact surface between fine sand and geogrid-layer in the transverse direction. Elias and Barry (2001) describe the factors affecting the shearing

resistance transmitted through the transverse-ribs. These factors are: friction angle, vertical stress, geogrid opening size and geogrid thickness, the reason for the transferred strength is the passive earth resistance that developed on the transverse-ribs.

### 3.3.1. Shear Strength

The shearing resistance in the transverse direction is described by the transversal shearing resistance percentage (TSSP), the TSSP value is defined as the percentage between the transverse shearing resistance and the longitudinal shearing resistance. The TSSP values increase with normal stresses and decrease with increasing geogrid-axial stiffness, as shown in Figure (10). The TSSP values for the geogrid-axial stiffness of 200 kN/m and the fine-sand elastic modulus of 10 MPa are 10.99, 21.24, 31.67 and 26.85% when the normal stresses are 25, 50, 75, and 100 kPa, respectively. When the fine-sand elastic modulus increases to 40 MPa, the TSSP values are 7.73, 7.61, 11.32 and 12.43%. In general, average TSSP values are between 5% and 25% for an elastic modulus of 10 MPa and between 4% and 15% for an elastic modulus of 40 MPa. The use of a biaxial geogrid-layer allows stress distribution in both longitudinal and transverse directions. The more effective TSSP values occur at low values of the fine-sand elastic modulus and geogrid-axial stiffness.
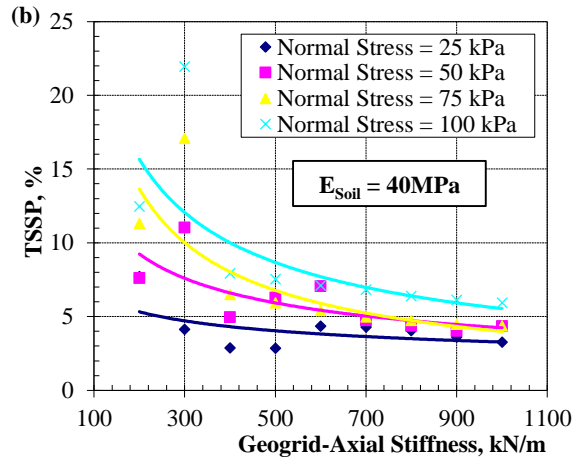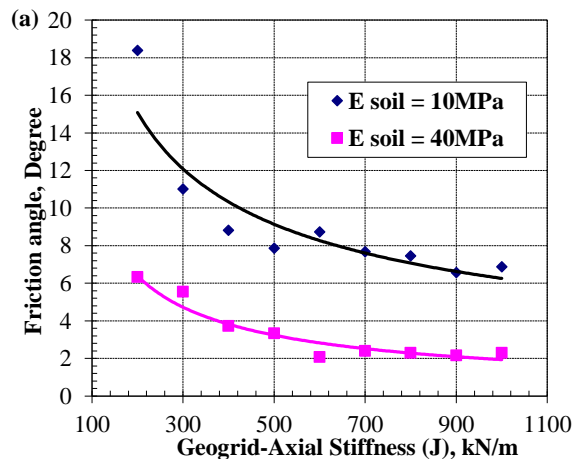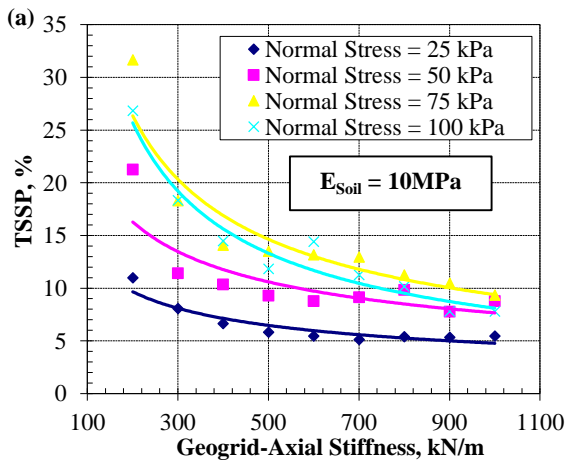
Fig. 10. Shear Strength percent versus Geogrid-Axial Stiffness in Transverse Direction

### 3.3.2. Shear Strength Parameters

Figure (11) describes the shearing resistance parameters versus geogrid-axial stiffness developed in the transverse direction. The results show that the friction angle between the fine sand and the geogrid-layer at the contact surface is twice as large at a fine-sand elastic modulus of 10 MPa than at a fine-sand elastic modulus of 40 MPa. The results illustrate that the transverse shearing resistance depends on the friction angle and there is no mobilized cohesion in the transverse direction for two cases of fine-sand elastic moduli.
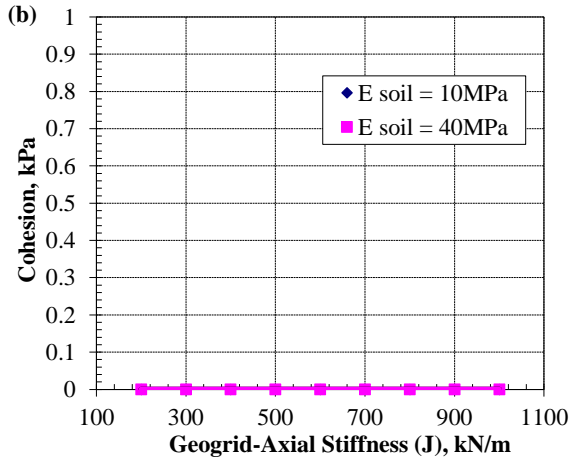
Fig. 11. Shear Strength Parameters versus Geogrid-Axial Stiffness in Transverse Direction



Fig. 12. Shear Strength Ratio (SSR) versus Geogrid-Axial Stiffness in Transverse Direction.

### 3.3.3. Shear strength Ratio

The shear strength ratio is the ratio (SSR) between the shearing resistance transmitted in the transverse direction of geogrid-reinforced fine sand and the shearing resistance of unreinforced fine sand. The results show that the SSR decreases with increasing geogrid-axial stiffness for different values of fine-sand elastic modulus and increases with the applied normal stresses as shown in Figure (12). In general, the increase in (SSR) value is 2.50 times with an increase in normal stress from 25 kPa to 100 kPa. In addition, by increasing the fine-sand elastic modulus from 10 MPa to 40 MPa, the (SSR) value increases by 2.0 times.
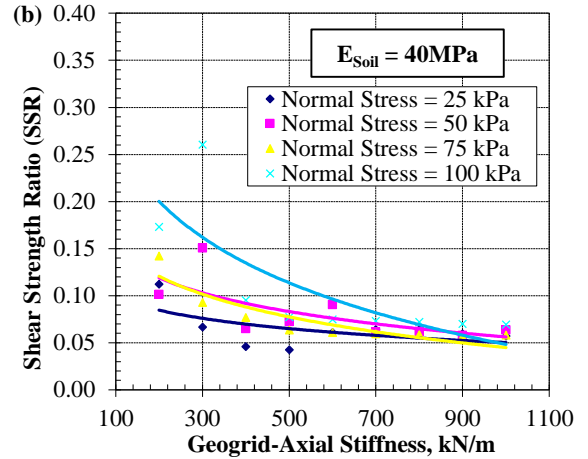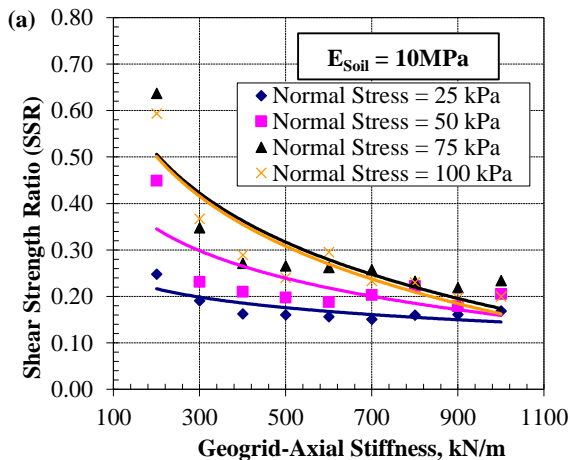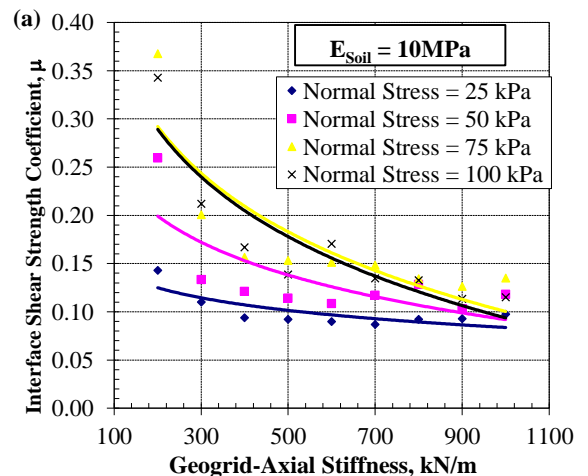
### 3.3.4. Interface Shear Strength Coefficient

Figure (13) shows the relationship between the interface shearing resistance coefficient mobilized in the transverse direction and the geogrid-axial stiffness. The results illustrate that the interface shearing resistance coefficient mobilized in the transverse direction decreases with increasing geogrid-axial stiffness for the two cases of fine-sand elastic modulus and increases with normal stresses. The percentage between the interface shearing resistance coefficient in the transverse and longitudinal directions at normal stress of 25 kPa and geogrid-axial stiffness of 500 kN/m is 7.0% and 5.0% for the fine-sand elastic modulus of 10 MPa and 40MPa respectively. in addition, the value of the interface shearing resistance coefficient of the fine-sand elastic modulus of 10 MPa is about 2.50 times when the fine-sand elastic modulus increases to 40 MPa.
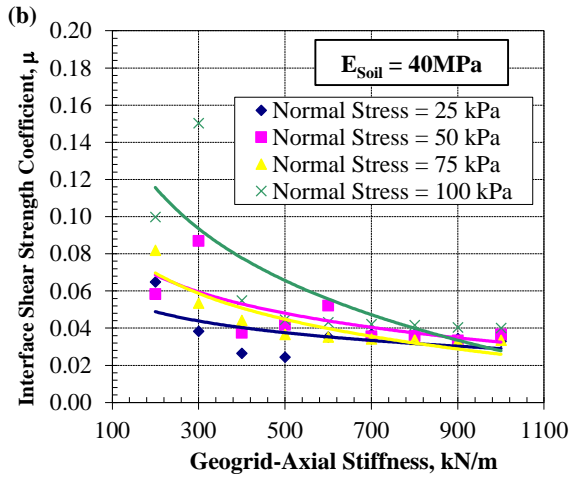
Fig. 13. Interface Shear Strength Coefficient versus Geogrid-Axial Stiffness in Transverse Direction.

*3.3.5. Mobilized Geogrid Tensile Strength*

Figure (14) shows the mobilized axial strength within the geogrid-ribs in the transverse direction. The results illustrate that the mobilized axial strength increases with geogrid-axial stiffness and the normal stresses for the two cases of fine-sand elastic modulus. The values of mobilized axial strength are 1.16 and 3.06 for geogrid-axial stiffness of 200 kN/m and 1000 kN/m, respectively, when the normal stress is 100 kPa and the fine-sand elastic modulus is 10 MPa, while these values decrease to 0.63 and 1.31 kN/m due to the increasing of fine-sand elastic modulus to 40 MPa. Furthermore, the percentage of mobilized axial strength in the transverse direction is about 10 to 18% of mobilized axial strength in the longitudinal direction.
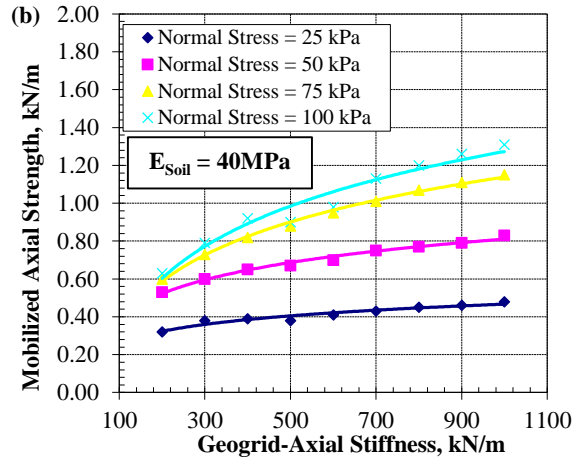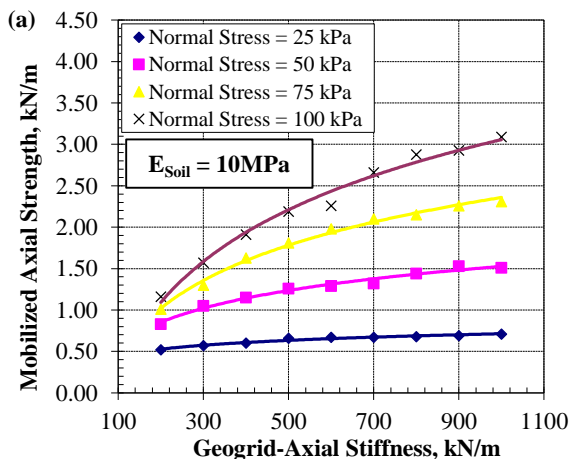




Fig. 14. Mobilized Geogrid Axial Strength versus Geogrid-Axial Stiffness in Transverse Direction.

## 4. Conclusions

The study presents a numerical simulation of a large-scale direct shearing test to investigate the effect of the geogrid-axial stiffness on the shearing resistance behavior of fine sand with different values of elastic modulus reinforced with geogrid-layer in both longitudinal and transverse directions. The following are the specific conclusions of the parametric study:

- The numerical results of the simulation model agree well with the experimental study for the shearing resistance of unreinforced and reinforced sand.

- The shear strength of reinforced fine-sand increases with the geogrid-axial stiffness; increasing shear strength is more efficient at low values of fine-sand elastic modulus.

- In the longitudinal-direction, for a fine-sand elastic-modulus of 10 MPa, the average shear strength increased from 2.0 to 2.50 times when the geogrid-axial stiffness varied from 200 kN/m to 1000 kN/m. When the fine-sand elastic-modulus was 40 MPa, these values increased from 1.27 to 1.36 times.

- In the transverse direction, the average transverse shear resistance percentage (TSSP) decreased from 25% to 5.0% when the geogrid-axial stiffness varied between 200 kN/m and 1000 kN/m when fine-sand elastic-modulus was 10 MPa. With a fine-sand elastic-modulus of 40 MPa, these values also decreased from 15% to 4.0%.

- In the longitudinal direction, the average friction angle decreased from 51° to 44.3° for a fine-sand

elastic-modulus of 10 MPa when the geogrid-axial stiffness varied from 200 kN/m to 1000 kN/m. With a fine sand elastic modulus of 40 MPa, these values decreased from 38° to 26.57°.

- In the transverse direction, for a fine-sand elastic-modulus of 10 MPa, the average mobilized friction angle decreased from 18.38° to 6.4° for the variation of geogrid-axial stiffness from 200 kN/m to 1000 kN/m. A fine-sand elastic-modulus of 40 MPa, these values decreased from 6.87° to 2.3°. No adhesion mobilized for both cases of E = 10 MPa and E = 40 MPa.

- In the longitudinal direction, for a fine-sand elastic-modulus of 10 MPa, the average interface shear strength coefficient (μ) increased from 1.28 to 1.78 when the geogrid-axial stiffness varied from 200 kN/m to 1000 kN/m. For a fine-sand elastic-modulus of 40 MPa, these values increased from 0.84 to 1.01.

- In the transverse direction, when a fine-sand elastic-modulus of 10 MPa and the variation of geogrid-axial stiffness from 200 kN/m to 1000 kN/m, the average mobilized interface shear strength coefficient (μ) decreased from 0.25 to 0.10 while these values decreased from 0.10 to 0.03 when the fine-sand elastic-modulus increased to 40 MPa,

- In the longitudinal direction, the average mobilized geogrid axial strength increased from 9.16 to 18.0 kN/m when the varying of geogrid-axial stiffness increased from 200 kN/m to 1000 kN/m at a fine-sand elastic-modulus of 10 MPa. these values increased from 11.6 to 40 kN/m when a fine-sand elastic-modulus of 40 MPa.

- In the transverse direction, for a fine-sand elastic-modulus of 10 MPa, the average mobilized geogrid axial strength increased from 1.0 kN/m to 2.0 kN/m when the varying of geogrid-axial stiffness increased from 200 kN/m to 1000 kN/m. For a fine-sand elastic modulus of 40 MPa, these values increased from 0.50 kN/m to 1.0 kN/m.

- In order to minimize the cost of the soil reinforcement process, the more economical and optimal values of geogrid-axial stiffness are 500 kN/m and 300 kN/m for fine-sand elastic moduli of 10 MPa and 40 MPa, respectively.

## References

[1] Ahad B. K. and Ali A. M., "Numerical and experimental direct shear tests for coarse grained soils", Chinese Society of Particuology and Institute of Process Engineering, Volume 7, Issue 1, pp. 83-91, 18 February 2009. DOI:10.1016/j.partic.2008.11.006

[2] Tamassoki S., Moayed R. Z., Ashkani M. and Rahimi H., "Scale Effect on the Shear Strength of Two-Layer Soil Reinforced by Geogrid", Malaysian Journal of Civil Engineering, Volume 30, No. 1, pp. 113-127, 2018. DOI: https://doi.org/10.11113/mjce.v30.15721

[3] Liu C., Zornberg J.G., Chen T-C., Ho Y. and Lin B., "Behavior of Geogrid-Sand Interfaces in Direct Shear Mode", Journal of Geotechnical and Geoenvironmental Engineering (ASCE), Vol. 135, No. 12, pp. 1863-1871, December 2009. http://dx.doi.org/10.1061/(ASCE)GT.1943-5606.0000150

[4] Tiwari N. and Satyam N., "Performance Evaluation of Reinforced Expansive Soil Subgrade with Polypropylene Fiber and Geogrid", Advances in Transportation Geotechnics, Volume IV, pp. 545-557, 2022. https://doi.org/10.1038/s41598-022-10773-0

[5] Stacho J., Sulovska M. and Slavik I., "Determining the Shear Strength Properties of a Soil-geogrid Interface Using a Large-scale Direct Shear Test Apparatus", Periodica Polytechnica Civil Engineering, Volume 64, Issue 4, pp. 989-998, 2020. https://doi.org/10.3311/PPci.15766

[6] Ferreira F. B., Vieira C.S. and Lopes M. L., "Direct Shear Behavior of Residual Soil-Geosynthetic Interfaces-Influence of Soil Moisture Content, Soil Density and Geosynthetic Type", Geosynthetics International, Volume 22, Issue 3, pp. 257-272, June 2015. DOI: 10.1680/gein.15.00011

[7] Makkar F.M., Chandrakaran S. and Sankar N., "Performance of 3-D Geogrid-Reinforced Sand under Direct Shear Mode", International Journal of Geotechnical Engineering, Volume 13, Issue 3, pp. 227-235, 2017. Https://doi.org/10.1080/19386362.2017.1336297

[8] Elkorashi I. A., El-Sideek M. B., Hassan A. R., Mowafy Y. and Farouk A., "Experimental And Numerical Study of the Isometric Cogged Biaxial Geogrid (ICB-GGR)", Journal of Al-Azhar University Engineering Sector, Volume 15, No. 57, pp. 1052-1063, October 2020. https://DOI: 10.21608/AUEJ.2020.120365

[9] Elias V., Barry P. and Christopher R., "Mechanically Stabilized Earth Walls and Reinforced Soil Slopes Design and Construction Guidelines: FHW", March 2001.

[10] Park S.S. and Byrne P.M., "Stress densification and its evaluation", Canadian Geotechnical Journal, Volume 41, Number 1, pp. 181–186, 2004. https://doi.org/10.1139/t03-076

[11] Anubud L., Jaroonrat P., Ayawanna J., Naebpetch W. and Chaiyaput S., "Evaluation of Interface Shear Strength

Coefficient of Alternative Geogrid Made from Para Rubber Sheet”, Polymers journal, Volume 15, Issue 7, 2023.
https://www.mdpi.com/2073-4360/15/7/1707

[12] Abaqus/CAE User's Guide, Version 6.14, United State of America, 2014.
http://130.149.89.49:2080/v6.14/

[13] Helwany S., “Applied Soil Mechanics With ABAQUS Applications”, John Wiley & Sons, 2007. ISBN: 978-0-471-79107-2.